Erschienen in: Macromolecular Bioscience ; 18 (2018), 6. - 1800018
https://doi.org/10.1002/mabi.201800018

Ionic Dependence of Gelatin Hydrogel Architecture Explored Using Small and Very Small Angle Neutron Scattering Technique

*Baohu Wu, Maria Siglreitmeier, Christian Debus, Dietmar Schwahn, Helmut Cölfen, and Vitaliy Pipich**

The hierarchical structure of gelatin hydrogels mimics a natural extracellular matrix and provides an optimized microenvironment for the growth of 3D structured tissue analogs. In the presence of metal ions, gelatin hydrogels exhibit various mechanical properties that are correlated with the molecular interactions and the hierarchical structure. The structure and structural response of gelatin hydrogels to variation of gelatin concentration, pH, or addition of metal ions are explored by small and very small angle neutron scattering over broad length scales. The measurements of the hydrogels reveal the existence of a two-level structure of colloid-like large clusters and a 3D cage-like gel network. In the presence of Fe^{3+} ions the hydrogels show a highly dense and stiff network, while Ca^{2+} ions have an opposite effect. The results provide important structural insight for improvement of the design of gelatin based hydrogels and are therefore suitable for various applications.

1. Introduction

Metal ions play an essential role for the function of biomacromolecules (e.g., protein, DNA) which are implicated in a wide range of physiological process including ion signaling control,[1] muscle contraction,[2] enzyme interactions,[3] etc. Unlike in salt solutions, some metal ions are confined to the biomacromolecule surface and can be accumulated in large number upon biomacromolecule organization. Thus, a study of structural aspects of ion/biomacromolecular interaction has the potential to contribute to a more comprehensive understanding of ion mediated structural organization of biomacromolecules within the extracellular matrix.

Gelatin is a water-soluble polypeptide derived from insoluble collagen through hydrolysis. The fibrous collagen molecule is formed by three individual protein strands and has the conformation of a triple helix.[4] Collagen extracted from skin and bones is composed of α-chains with molar mass ≈95 kDa, width ≈1.5 nm and length ≈300 nm.[5] Hydrolysis separates the collagen triple helix into three protein strands decomposing to gelatin. Each protein strand with left-handed proline helix conformation contains between 50 and 1000 amino acids.[6] Gelatin molecules in aqueous solution exhibit various conformations, which depend on the environmental conditions, such as the concentration, pH, temperature, and ionic strength.[7] An aqueous solution of 0.5–50 wt% gelatin above 40 °C is in a sol state and forms after cooling a thermoreversible gel due to the recovery of collagen-like right-handed triple helices via a transition from a random coil to triple-helix conformation.[8] Those hydrogels are built by a hierarchical assembly of many gelatin molecules (strands or filaments) in the range from few nanometers to several micrometers. The interaction between gelatin molecules in the gel network is usually driven by hydrogen bonding, hydrophobic forces, and electrostatic forces.[9–11] The addition of salt or other small dissolved components could change the interactions between gelatin molecules, thereby leading to structural reorganization. Generally, gelatin hydrogels are attractive soft materials for biological applications[12–14] owing to their various functional groups ($-NH_2$, $-COOH$), biocompatibility[15–17] and cavities inside the hydrogel protein scaffold. As a soluble polypeptide, gelatin molecules contain many carboxylic acid groups that can form ionic bonds in the presence of metal ions influencing the architecture of the gelatin gel network.[18] Moreover, we have found that metal ions strongly influence the conformation, the thermal stability, as well as mechanical properties of gelatin molecules. Although gelatin hydrogels as well as the modified hydrogels have been extensively studied,[1,4,5,18–24] there are only a few reports on the influence of ions on the structure and mechanical properties of gelatin hydrogels.[18]

Dr. B. Wu, Dr. V. Pipich
Jülich Centre for Neutron Science (JCNS) at
Heinz Maier-Leibnitz Zentrum (MLZ)
Forschungszentrum Jülich, Lichtenbergstr. 1
85748 Garching, Germany
E-mail: v.pipich@fz-juelich.de
Dr. B. Wu, Dr. M. Siglreitmeier, C. Debus, Prof. H. Cölfen
Department of Chemistry, Physical Chemistry
University of Konstanz
Universitaetsstr 10, Konstanz 78457, Germany
Dr. D. Schwahn
Forschungs-Neutronenquelle Heinz Maier-Leibnitz (FRM II)
Technische Universität München
Lichtenbergstr 1, Garching 85748, Germany

As in case of a typical physical gel, the mechanical properties of gelatin hydrogels are based on the assumption of a 3D, porous, interconnected network.[25] The architecture of the hydrogels on the length scale from 1 nm to several μm has strong impact on their mechanical properties. Limited information is known about the 3D original structure of gelatin hydrogels from microscopy methods.[22] To help understanding the interactions of biomolecules and biomolecular organization, we explored the structure and mechanical properties of gelatin hydrogels within a broad length scale by using small angle neutron scattering/very small angle neutron scattering (SANS/VSANS), swelling, as well as rheology. As an important nondestructive technique for the determination of the structure of length scales from nanometer to several micrometers, an in situ SANS/VSANS measurement provides information about the effect of structure on mechanical properties.[23,26] In this work, we have applied SANS/VSANS to study the structural response of gelatin hydrogels on gelatin concentration, pH, particularly affected by the metal cations Na^+, Ca^{2+}, and Fe^{3+}. We found that hydrogels represent quite different mechanical properties with various metal ions. The increase in the elastic modulus of the hydrogel was accompanied by an enhancement of fraction of triple helices in the presence of Fe^{3+}. In contrast, Ca^{2+} ions are lowering the gel elastic modulus due to decreasing the triple helices in the hydrogels. These features were attributed to the stronger interaction between metal ions and gelatin polypeptide strands, which impacts the formation of a stiffer structure. The established structure–property relationships have important implications for the design and use of gelatin hydrogels.

2. Experimental Section

2.1. Materials and Methods

2.1.1. Synthesis of Gelatin Hydrogels

Materials: Gelatin Type B (≈225 Bloom, Sigma-Aldrich), 4-chloro-*m*-cresol (Fluka), methanol (VWR), D_2O (99.8 at% D, ARMAR Chemicals), $CaCl_2$ (Sigma-Aldrich), NaCl (Sigma-Aldrich), $FeCl_3 \cdot 6H_2O$ (Sigma-Aldrich), DCl (35 wt% in D_2O, 99 at% D, Sigma-Aldrich), NaOD (40 wt% in D_2O, 99.5 at% D, Sigma-Aldrich) were used.

Different amounts of gelatin were allowed to swell in water for 24 h at 5 (±1)°C. Homogeneous solutions were prepared by heating the gels for 2 h at 45 °C. In each case, ≈0.7 mL of solution was filled into a quartz cell waiting for cool down to room temperature 20 (±2)°C. To avoid decomposition by bacteria, a 5 *wt*% solution of 4-chloro-*m*-chresol in methanol was added. The hydrogel samples were stored at 5 (±1)°C before the measurements. All the samples for SANS/VSANS measurements were prepared in D_2O or a mixture of D_2O and H_2O. The metal ions were introduced into gelatin hydrogels by either direct addition in the gel synthesis process (Na^+, Ca^{2+}) or soaking the hydrogels in ion (0.3 M Fe^{3+}) containing solutions at 5 (±1)°C.

2.1.2. SANS and VSANS Experiments

SANS and VSANS experiments were carried out at, respectively, the KWS-1[27] and KWS-3[28] diffractometers operated by the Jülich Centre for Neutron Science (JCNS) at the Heinz Maier-Leibnitz Zentrum in Garching, Germany. Four configurations were used at KWS-1, namely the sample-to-detector distances of 1.3, 2, 8, and 20 m, the collimation length of 8 and 20 m, and wavelength of 7 Å ($\Delta\lambda/\lambda$ = 10%). These settings allowed covering a Q-range from 0.002 to 0.35 $Å^{-1}$. A 2D position sensitive detector was used to detect neutrons scattered from the samples. In order to cover a larger length scale of the network structure, very-small angle neutron scattering experiments were carried out at the KWS-3 diffractometer using a parabolic mirror as an optical element, and covering the smaller Q range from 0.0001 to 0.0025 $Å^{-1}$.[28] Hydrogels were filled into rectangular quartz cells with path length of 1 or 2 mm. Plexiglas was used as a secondary standard to calibrate the scattering intensity in absolute units at KWS-1[27] and the direct beam method was used at KWS-3.[28] The data correction and calibration were performed using the software QtiKWS.[29] Fitting the SANS/VSANS data was done using software modules provided by JCNS *QtiKWS and National Institute of Standards and Technology (NIST) Igor*[30] analysis packages.

2.1.3. Differential Scanning Calorimetry (DSC)

Solid melting of gelatin hydrogel samples was measured by differential scanning calorimetry (DSC 8500, Perkin Elmer).

2.1.4. Rheological Experiments

Rheological properties of gelatin hydrogels (18 wt% in D_2O) were measured on an Anton Paar Modular Compact Rheometer (Physica MCR501) with 25 mm diameter parallel plate geometry and 0.05 mm gap distance. The rheometer was equilibrated at 20 °C prior to sample loading. Frequency (ω) sweep experiments were performed with strain being 0.8%. Dynamic sweep experiments were performed in order to determine the storage modulus (G') and loss modulus (G'') as a function of ω.

2.1.5. Swelling Experiments

The gelatin hydrogels were immersed in deionized water, 0.1 M NaCl, 1 M NaCl, 0.1 M $CaCl_2$, 1 M $CaCl_2$, and 0.3 M $FeCl_3$ solutions at room temperature (20 ± 2 °C), respectively. Before weighing, the excess water of each sample was removed with a tissue paper. All samples were weighed after a certain amount of time until equilibrium swelling was reached. The mass-based swelling degree (S_d) of the investigated gels is given by the following equation

$$S_d = \frac{W_s - W_0}{W_0} \times 100\% \quad (1)$$

where W_s is the weight of the swollen sample at a certain time and W_0 is the initial weight of the sample.

2.2. Theory

2.2.1. Small Angle Neutron Scattering

The SANS and VSANS diffractometers deliver scattering data from very small Q of the order of 10^{-4} up to 0.35 Å^{-1}, covering length scales from about 20 Å up to 6 µm. Q is the scattering vector where $Q = 4\pi sin\theta/\lambda$ is determined by the scattering angle 2θ and the neutron wavelength λ. Some scattering laws applicable for hydrogels are described in the following parts.

2.2.2. The Beaucage Expression

The Beaucage empirical expression is able to reasonably approximate the scattering from many different types of particles, including fractal clusters, random coils (Debye equation), ellipsoidal particles, etc.[31] The Beaucage expression is given according to

$$\frac{d\Sigma}{d\Omega}(Q) = \frac{d\Sigma}{d\Omega}(0)\exp(-u^2/3) + P_a[(erf(u/\sqrt{6}))^3/Q]^{\alpha} \quad (2)$$

representing a combination of Guinier's and Porod's law describing the scattering at low and large Q, respectively. More quantitatively both approximations are valid for the parameter $u = R_gQ$ smaller or larger than 1, u representing the product of the radius of gyration R_g and the scattering vector Q. Guinier's law has the shape of a Gaussian function whereas for Q larger than $1/R_g$ ($u > 1$), a power law according to $d\Sigma/d\Omega(Q) = P\alpha Q^{-}\alpha$ is contained. Those empirical expressions can also be used in a multilevel model for samples with a multiscale structure. In this paper, the scattering from a large inhomogeneous structure is fitted with the Beaucage expression to obtain size and fractal dimension of the gelatin structure.

2.2.3. The Fractal Cylinder Model

In the case of dense gelatin hydrogels, in which most of the gel networks are constructed by rigid rod-like triple-helices, the high Q scattering can be well described by the fractal-cylinder model.[32,33] The structure factor for a fractal network of spherical aggregates was proposed by Texeira[34] and has been applied for rod-like structures by Justice et al.[32] The model is a combination of a cylinder form factor $F(Q)_{cyl}$ and a fractal structure factor $S(Q)_{fractal}$

$$S(Q, D_f, \Xi, r_0) = 1 + \frac{D_f \exp(\Gamma(D_f - 1))\sin(D_f - 1)\tan^{-1}(Q\Xi)}{(Qr_0)^{D_f}[1 + (Q\Xi)^{-2}]^{(D_f-1)/2}} \quad (3)$$

where $\Gamma(x)$ is the gamma function, r_0 is the gauge of the measurement and Ξ gives the size of the fractal. The mass fractal dimension D_f is the power law exponent. The final equation for data fitting combines the form factor and the structure factor normalized with the contrast, volume fraction (ϕ), volume of the particles (V_p), and background (BKG) and can be written as

$$\frac{d\Sigma}{d\Omega}(Q) = \phi V_p(\Delta\rho)^2 P(Q)_{cyl} S(Q)_{fractal} + BKG \quad (4)$$

2.2.4. The Correlation Length Model

The scattering from gelatin molecules and their clustering effect is well described by the empirical functional model developed by Hammouda et al.[35]

$$\frac{d\Sigma}{d\Omega}(Q) = \frac{A}{Q^n} + \frac{C}{1 + (Q\xi)^m} + BKG \quad (5)$$

In this equation, a scattering of the gelatin network is described by the first term A/Qn and is qualitatively similar to Porod-like scattering that usually is used to evaluate the clustering strength of the primary scattering objects. Scattering at larger Q is expressed by the second term $C/[1 + (Q\xi)^m]$ and has been used to characterize the polymer/solvent interaction and chain solvation characteristics.[35] The correlation length ξ represents a weighted average of interdistances between the gelatin molecules. In this paper, it identifies the gelatin morphology and the structure on the nanoscale. The amplitudes of the Porod and Lorentzian terms (A and C, respectively), and the Porod and Lorentzian scattering exponents (n and m, respectively) were obtained by a nonlinear least-squares fit of the data.

3. Results and Discussion

The gelatin Type B used in the experiments has a molar mass of approximately 25–50 kDa. The thermal treatment ($T \approx 45$ °C) occurs in the presence of water (D_2O or H_2O) and is necessary in order to reduce both hydrogen and electrostatic interactions. After cooling down below 30 °C (see Figures S1 and S2, Supporting Information), the gelatin chains undergo a progressive conformational change of coil-to-helix transition.[8] As a result, a thermoreversible gel[36] is formed accompanied by a progressively increasing solution viscosity. Such a sol–gel transition occurs due to the formation of triple helices, by which are based on polypeptide intermolecular hydrogen bonds between carbonyl oxygen and amide hydrogen. At the same time, gelatin loses its solubility at cooling owing to the coil-to-helix transition.[37]

3.1. The Multiscale Structure of Gelatin Hydrogels

The structure of the hydrogel of various gelatin concentrations between 6 and 30 wt% in D_2O was determined by SANS and VSANS methods at room temperature (see **Figures 1** and **2**). The scattering cross-section of the investigated samples was obtained within the Q-range from 10^{-4} up to 0.35 Å^{-1}, covering length scales from 10 Å up to 6 µm.

In Figure 1 the scattering cross-section of 18 wt% gelatin in D_2O is shown. The scattering curve could be divided into two regimes separated by the so-called "knee point" at $Q_c \approx 0.025$ Å^{-1}.

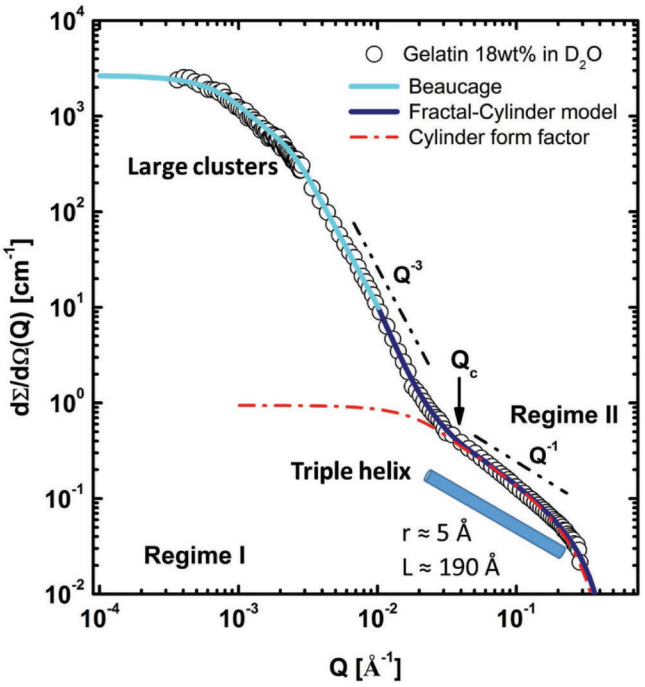

Figure 1. SANS/VSANS scattering profile of 18 wt% gelatin in D_2O is measured at $T = 20 \pm 2$ °C. The light-blue solid line ($Q > 0.01$ Å^{-1}) represents fitting by Equation (2) (Beaucage expression). The dark-blue solid line ($Q < 0.01$ Å^{-1}) represents fitting by Equations (3) and (4) (fractal cylinder model). The dashed-dotted-red line represents a cylinder form factor with a polydispersity of 0.2. The right bottom inset picture is a cylinder model for gelatin triple helix.

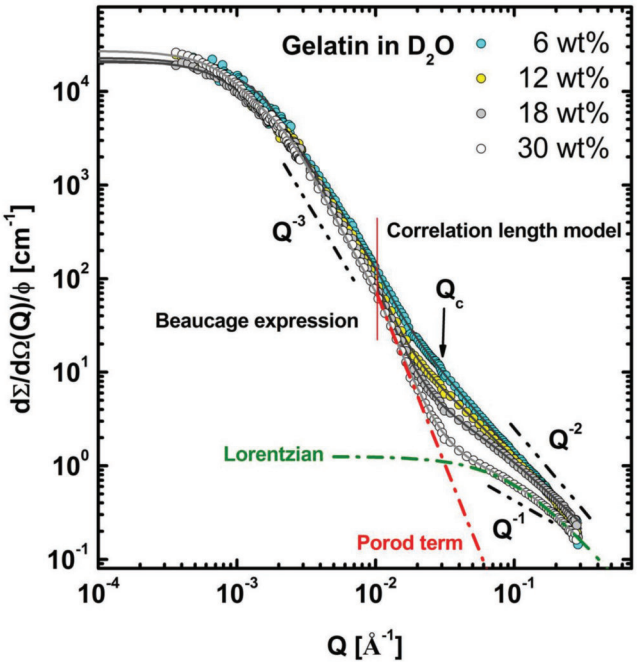

Figure 2. SANS/VSANS scattered intensity versus scattering vector Q for gelatin in D_2O as a function of gelatin concentration ($T = 20 \pm 2$ °C). The scattering cross-section was normalized with gel volume fraction, φ. At low Q (<0.002 Å^{-1}), VSANS data are also presented after rescaling. The solid lines represent the fitting by the Beaucage model (Equation (2), $Q < 0.01$ Å^{-1}) and correlation length model (Equation (5), $Q > 0.01$ Å^{-1}).

Scattering from large gelatin clusters dominates within "Regime I" ($Q < Q_c$), whereas "Regime II" ($Q > Q_c$) reveals information from the internal gelatin structure. The scattering below 0.01 Å^{-1} within "Regime I" shows a Guinier profile of a large-scale inhomogeneous structure. This scattering is well described by the light-blue-line representing the best fit of the data using the Beaucage expression[31] (Equation (2)) with radius of gyration of $R_g = 1590 \pm 30$ Å and fractal dimension $\alpha \approx 2.7$. The forward scattering $d\Sigma/d\Omega(0)$, amplitude of the Porod's law P_α, as well as other parameters of the fits are presented for samples with different gelatin concentration in Figure 2 and Table S1 in the Supporting Information.

A possible multiscale structure of a reconstructed gelatin hydrogel is shown in **Figure 3**. In Figure 3a is a model showing the large clusters with a dense inner phase and a loose surface. The scattering curve above 0.01 Å^{-1} follows two power laws namely a crossover from $Q^{-}1$ (higher Q part) to $Q^{-}3$ (lower Q part in the "Regime II") as Q decreases. The crossover at Q_c tracks a change from a regime in which scattering from single rods dominates (at high Q) to one in which collective effects prevail (at low Q). Thereby for gelatin hydrogels, the scattering indicates domination of rod-like structure of gelatin helix bundles with fractal-like aggregation. At the crossover position Q_c, a length scale $R_m = 2\pi/Q_c$ could be considered as the 3D-cage size of the hydrogel network.

In case of the 18 wt% gelatin sample, most of the gel network is build up by rigid rod-like triple-helices. The high Q scattering ($Q > 0.01$ Å^{-1}) can be well described by the green solid lines representing the best fit of the fractal-cylinder model.[32,33] The obtained parameters of the fit (Equation (3)) are compiled in Table S1 in the Supporting Information. Inspection of the obtained values in Table S1 in the Supporting Information clearly indicates that long rod-like objects with a length of >190 Å and cross-section diameter of ≈9.8 Å aggregate to a mass fractal network. The value of the rod diameter is in fairly good agreement with the collagen triple-helix derived from crystallographic data as presented in Figure 3e. The characteristic length Ξ (Equation (3)) of ≈249 Å is very close to the value calculated from Q_c representing the size of the hydrogel 3D cage. Thus, the three characteristic length scales Ξ, 3D cage size R_m, and length of gelatin helices L are correlated with the crossover position Q_c.

3.2. Structure as a Function of Gelatin Concentration

It is well known that the mechanical properties of gelatin hydrogels depend on gelatin concentration. We therefore explored the hydrogel structure of several gelatin concentrations between 6 and 30 wt% as shown in Figure 2. In this figure, the scattering curves were normalized with gelatin volume fraction ϕ. The scattering from the large aggregates of all shown samples follows a master curve with approximately the same normalized forward scattering. The scattering from the local structure shows a continuous transition of the power low exponent from 2 to 1. This increase of the exponent could be explained

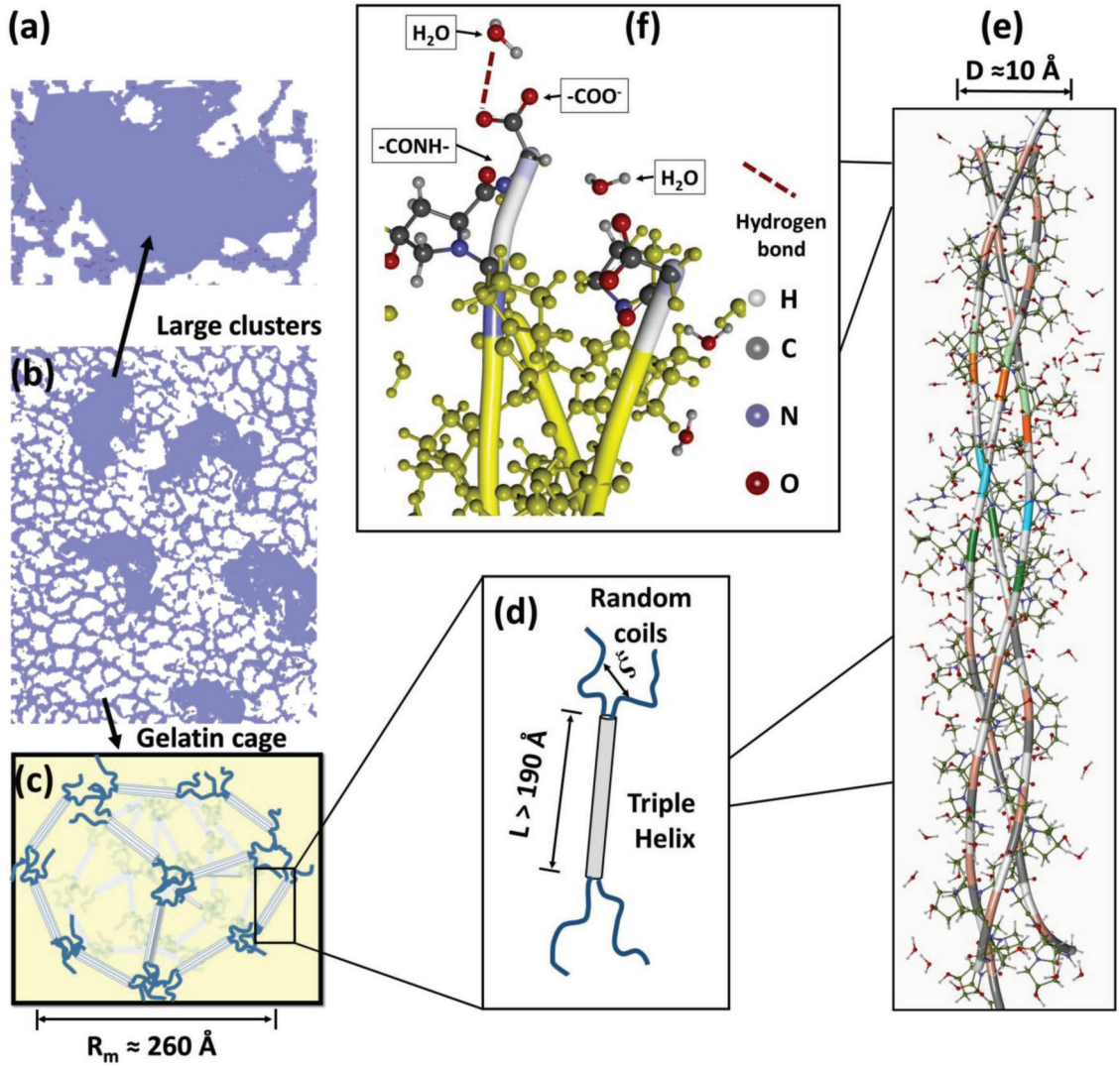

Figure 3. Schematic representation of the gelatin structure from larger scale to molecular level: a) Gelatin large clusters. b) Sketch of the gelatin hydrogel structure with large clusters and gel network. c) 3D Cage-like Gel matrix. d) Gelatin triple-helix and random coil. e,f) Macromolecular structure of a collagen-like triple-helical structure reconstructed from (Protein Database code 1BKV).[22]

by the conformational change of the gelatin molecules such as a transition from Gaussian-chain to triple helix conformation. The scattering data at the high Q range were fitted with the correlation length model (Equation (5)) as plotted by the solid line representations. The extracted parameters of both regimes are plotted in **Figure 4** and listed Table S2 in the Supporting Information, respectively.

In Figure 4 and Table S2 in the Supporting Information the concentration dependence of the "low-Q" cluster radius of gyration (R_g) and the "high-Q" polymer chain correlation length (ξ) for the gelatin samples at room temperature are compared. The radius of gyration increases with gelatin concentration from 1110 to 1700 Å. The scattering intensity at zero angle $d\Sigma/d\Omega(0)$ increases linearly with gelatin concentration. The SANS/VSANS results show a power law where α in "Regime I" slight increase with increasing gelatin concentration, from 2.5 to 2.7 for 6–30 wt% of gelatin, respectively. This implies that the gelatin network consists of large phase-separated domains (collapsed polymer coils) showing a surface fractal conformation with increasing concentration of gelatin.

From the data in Figure 4 and Table S2 in the Supporting Information, the correlation length ξ significantly decreases with gelatin concentration from 80 to 10 Å. An enhanced compactness of the network with concentration is related to an increase in the number of interaction points (hydrogen bonding interactions) and an associated reduction in the interchain (random coils) distance at these points. Moreover, the crossover at Q_c (sample Gelatin 18 wt% in D_2O of ≈0.024 Å^{-1}) allows to estimate the gelatin average 3D cage size of $R_m = 2\pi/Q_c \approx 258$ Å^{-1}. The average cage size of different samples seems independent on the concentration of gelatin hydrogels. The power law exponent β in the "Regime II" correlates with the gel concentration and decreases from 1.7 to 0.98 with increasing of the gelatin concentration. The trend to $\beta = 1$,

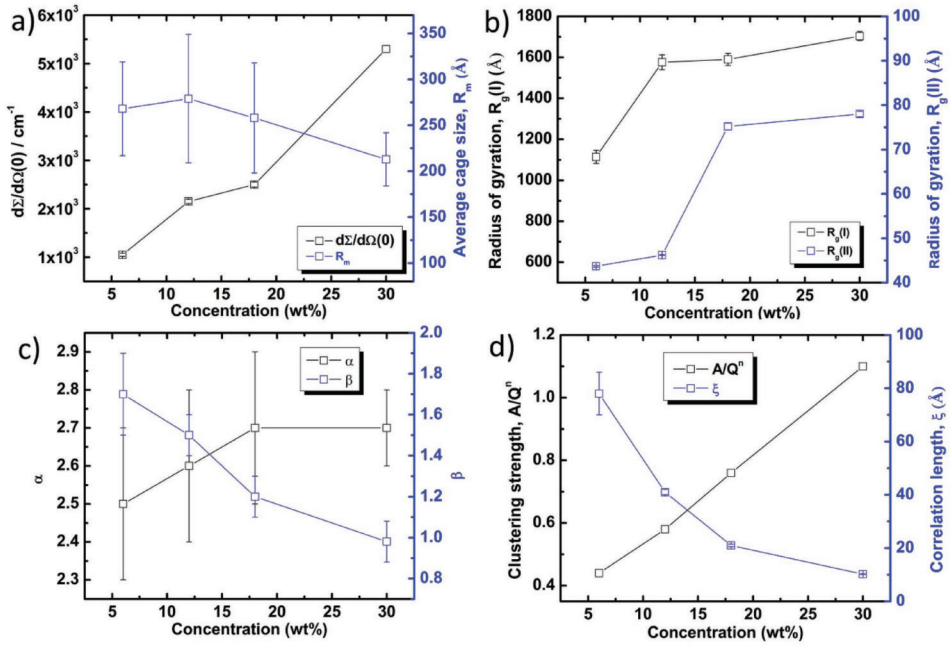

Figure 4. Parameters of gelatin hydrogels with different concentrations in D_2O obtained from the SANS/VSANS fitting results by Equations (2) and (5). a) Forward scattering $d\Sigma/d\Omega(0)$ and the average cage size of the hydrogels, R_m. b) Radius of gyration obtained from "Regime I," $R_g(I)$ and "Regime II," $R_g(II)$. c) The power law exponent at intermediate Q (α) and high Q (β). d) The clustering strength, A/Qn (Q = 0.02 Å^{-1}) and correlation length ξ.

i.e., scattering from rigid rod-like particles, indicates enhanced triple helix bundles.

The parameters of the clustering strength (A/Qn) for the "Regime II" are presented versus the gelatin concentration in Figure 4 and Table S2 in the Supporting Information. High clustering strength corresponds to networks while low clustering strength corresponds to dissolved chains. The intermediate case corresponds to branched structures. Thus, the higher concentration gelatin samples show network features (e.g., gelatin 30 wt% of 1.1) while lower concentration gelatin samples show a branched structure with partially dissolved chains in solution (e.g., gelatin 6 wt% of 0.44). Clustering and solvation increases and decreases, respectively.[38]

Thus, the SANS/VSANS results demonstrate the existence of two phases in pure gelatin gels: one consists of colloid-like clusters of densely packed gelatin molecules ("dense phase"); the other phase is formed as a 3D cage-like gel network composed of gelatin triple-helices and random coils ("dilute phase"). In the "dilute phase" the ratio between gelatin triple-helices and random coils is a function of gelatin concentration. On the small-scale structure level, SANS reveals the changes of the gelatin conformation which can results in changes in the overall gel strength. The correlation length ξ significantly decreases with increasing gel concentration and that corresponds to an increase in the number of interaction points. A conformational change is accompanied by changing the gel concentration and more rigid rod-like triple helix bundles have been found in concentrated gels. On the large-scale structural level, the number density of gelatin large clusters is proportional to the gel concentration.

3.3. The pH Effects on the Hydrogel Structure

The pH of the gelatin (Type B) hydrogels is about 5, varies slightly with concentration, and is close to the isoelectric point (IEP, pH = 4.7–5.3). Comparing with the other pH conditions, the viscosity and gel strength of Type B gelatin is at a minimum and maximum respectively with the pH around 5 reflecting the importance of the pH for rheological properties and thereby industrial applications.[39,40]

Figure 5a shows the effects of pH on the SANS/VSANS scattering profiles of gelatin hydrogels with pH around 5.1 (in D_2O), 3.4 (with 0.1 M DCl in D_2O), and 10.7 (with 0.1 M NaOD in D_2O). The pH of a sample in D_2O was recalculated by the pH meter reading (pH*) with the following relationship: pH = 0.929pH* + 0.42.[41] In the "Regime II" (Figure 5a), the SANS results show the same scattering in 0.1 M DCl in comparison with the sample in D_2O (pH ≈ 5.1). The large structure in Regime I increased in size between the values found for the two samples (from 1590 ± 30 Å of gelatin in D_2O to 2096 ± 60 Å of gelatin 0.1 M DCl, Table S3, Supporting information). Moreover, there is nearly no change of the crossover point, Q_c, indicating the same cage size in the two samples. Figure 5b displays the effects of higher pH of around 10.7 on the SANS/VSANS scattering profiles of gelatin hydrogels (gelatin in 0.1 M NaOD). Scattering shows a significant enhancement at the low Q of the power law exponent from almost 0 (Guinier regime) to ≈3 (fractal structure, see the inset of Figure 5b; as a result of a higher clustering strength factor, see Table S3, Supporting Information) revealing the large clusters in the sample. In "Regime II," scattering has a lower scattering

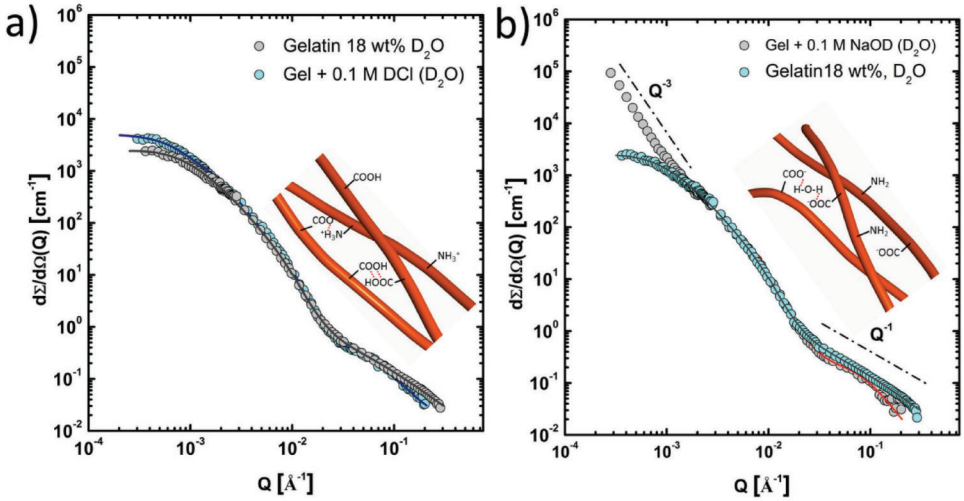

Figure 5. SANS/VSANS scattering cross-sections versus scattering vector Q for gelatin 18 wt% in D_2O with 0.1 M DCl a) and gelatin 18 wt% in D_2O with 0.1 M NaOD b). Gelatin 18 wt% in D_2O without turning the pH values (pH ≈ 5.1) was plotted for comparison. The solid lines represent the fitting by the Beaucage model (Equation (2), $Q < 0.01$ Å^{-1}) and correlation length model (Equation (5), $Q > 0.01$ Å^{-1}).

intensity indicating a lower amount of triple helices in the hydrogels.

The fitting parameters of SANS/VSANS in Table S3 in the Supporting Information show that the correlation length decreases from 25.0 to 13.8 Å and to 11.5 Å for the samples in D_2O, under acidic conditions, and under basic conditions, respectively. The change of the correlation length is accompanied by a change of the parameter C, which reflects declining amount of triple helices at a sample pH far away from the IEP. In gelatin molecules, the triple helices of native collagen are stabilized by two noncovalent interactions: hydrogen bonding and dipolar interactions. As the pH deviates from the isoelectric point, more polar groups such as $-COOH$, $-NH_2$ partly transform to their charged groups $-COO^-$(pH > IEP) and $-NH_3^+$ (pH < IEP) so that a majority of positive groups exists over the negative or vice versa depending on the pH value. Those changes are breaking the interaction between gelatin residues thus influencing the stability of gelatin triple helices. Therefore, either at much higher or lower pH than the IEP, gelatin hydrogels have less triple helix conformational units, thus leading to poorer mechanical properties.

3.4. Effect of Metal Ions on the Hydrogel Structure

Ions of salt could affect the gelatin structure via tuning the electrostatic interaction strength, the formation of salt bridges, hydration, and hydrogen bonding.[39] The influence of several salts on the SANS/VSANS scattering profile of 18 wt% gelatin in D_2O is shown in **Figure 6**. Chloride salts with cations of different valences, namely monovalent (Na^+), divalent (Ca^{2+}), and trivalent (Fe^{3+}) of different concentrations were added. The scattering profiles were fitted both with the Beaucage and correlation length model in Regimes I and II respectively. The extracted parameters are plotted **Figure 7** and listed in Table S4 in the Supporting Information. The scattering of the gelatin network shows various changes depending on the species and concentration of salts. The forward scattering $d\Sigma/d\Omega(0)$ of the clusters in "Regime I" increases after adding salt with monovalent NaCl 0.1 and 1 M in Figure 6a. Low Q scattering shows that the salt impact on the structure occurs without dramatically increasing the size instead of increasing the number density and/or contrast of the larger clusters. In Figure 6a "Regime II," the addition of monovalent ions Na^+ in the hydrogels does not show clear changes in the scattering in comparison to the salt-free gels (also see Figure 6d). A small reduction of R_g and the correlation length ξ is observed. However, the difference between the sample in 0.1 M NaCl and 1 M NaCl (with variable ionic strength) shows that the electrostatic interaction strength does not influence the interhelix interactions. At room temperature of 20 ± 2 °C, all of the gelatin samples with a large amount of NaCl (up to 2 M) are in the gel state. These results indicate that Na^+ ions have only a weak interaction with the gelatin molecules.

Divalent metal ions such as Ca^{2+}, Cu^{2+}, Zn^{2+}, and Co^{2+} play a different role in gelatin interhelix interactions in comparison with monovalent metal ions.[18,42] In nature, calcium ion–collagen interactions play an important role for bone tissue mineralization.[43] Those divalent metal ions can form ionic bonds with the carboxylic acid groups of the gelatin polypeptides, thereby influencing the organization of the gelatin network. In the inset of Figure 6d, we see that the addition of divalent cations decreases the scattering intensity when compared to the sample with Na^+ and without additional salts. The R_g of the samples with divalent ions becomes smaller and is around 2/3 of the salt-free hydrogels (Table S4, Supporting Information). This result is correlated with a smaller 3D-cage size of the gelatin network. From another side, increasing of Ca^{2+} ion concentration from 0.1 to 1 M significantly decreases the clustering strength A/Q^n. Thus, Ca^{2+} ions have the ability to deform the gelatin triple-helix gel network in the range of applied salt concentrations. The results are consistent with the phase behavior of the gelatin hydrogel in the presence of Ca^{2+} ions as the gel phase changes into the solution phase beyond a critical

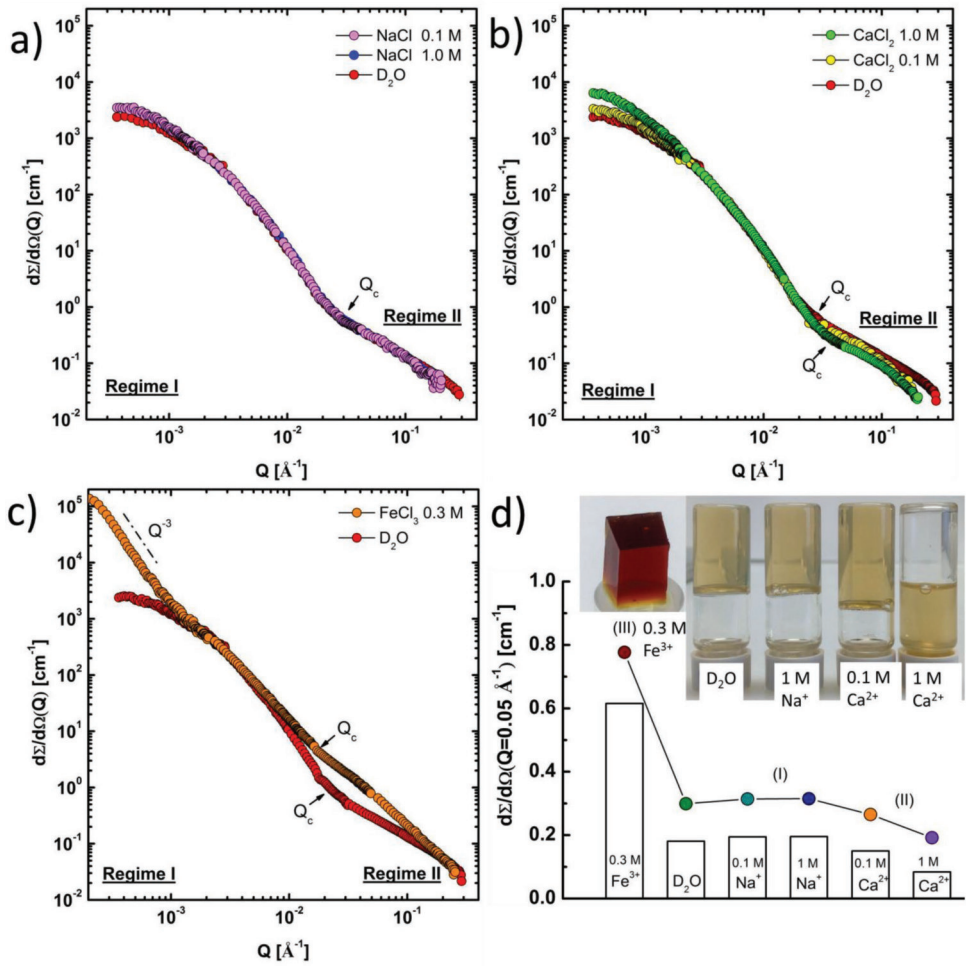

Figure 6. SANS/VSANS scattered intensity versus scattering vector Q for gelatin 18 wt% in D_2O and salt solutions with different concentration and counter ion valence. a) Gelatin 18 wt% in D_2O with additional 0.1 M NaCl and 1 M NaCl. b) Gelatin in D_2O with additional 0.1 M $CaCl_2$ and 1 M $CaCl_2$. c) Gelatin sample (18 wt%) swollen in 0.3 M $FeCl_3$ in D_2O. d) The plot represents the scattering intensity of samples at $Q = 0.05$ Å^{-1}. The insert pictures show the appearance of the ions-gelatin interactive samples.

concentration of 0.9 M Ca^{2+} (at 20 °C). In the presence of 1 M Ca^{2+} (at 20 °C), the gelatin has been transformed into a solution phase indicating that the Ca^{2+} ions have a strong influence on the gelation properties (inset picture of Figure 6d).

The stabilization or destabilization effects induced by salts in driving conformation transitions of macromolecules are following the well-known Hofmeister series.[44,45] Sodium chloride ions have only minor influence on the structure of gelatin hydrogels even at a very high concentration (1.3 M). In the presence of calcium chloride, the interaction of Ca^{2+} cations and carboxylic acid groups of the gelatin polypeptide deteriorate the cohesion of the triple helix constituents results a relatively soft structure. An early study shows that the ion-peptide group interaction plays an important role on gelation.[46] Calcium-carboxylic ligand complexes in a Ca^{2+}-gelatin solution inhibit triple helix formation and thus gelation of the gelatin macromolecules. The inhibition of the triple helix formation is due to the calcium-peptide complex but not to the side chain. Thus at concentrations above 0.9 M of Ca^{2+} cations, 18 wt% gelatin solution contains enough calcium ion-peptide complexes inhibiting the triple helix formation to suppress gelation (at 20 °C).

In "Regime I" (Figure 6c), trivalent cations, Fe^{3+} indicate a strong effect of aggregation of large gelatin clusters as evident in the lower Q scattering (power law exponent of 3). In "Regime II," the Fe^{3+} ions stimulate a significant increase of the scattering intensity in conjugation with a dramatically enhanced R_g, clustering strength, and 3D-cage size. These changes indicate formation of a larger number of triple helices and aggregation of triple helices (increasing the rod-like species diameter). Therefore, the Fe^{3+} ions show a strong crosslinking effect on the gelatin network, which leads to additional junctions of the gelatin chains in between the triple helical crosslinks. When compared with divalent cations, the binding strength of trivalent cations with gelatin is strongly enhanced. It is important to note that the trivalent Fe^{3+} ions could interact with three carboxylic acid groups of different chains,[47] thus serving as a coordination center for triple helices. So, it is possible to form more gelatin triple-helices in the presence of Fe^{3+}. Furthermore, introducing Fe^{3+} to the gelatin hydrogel yielded an additional

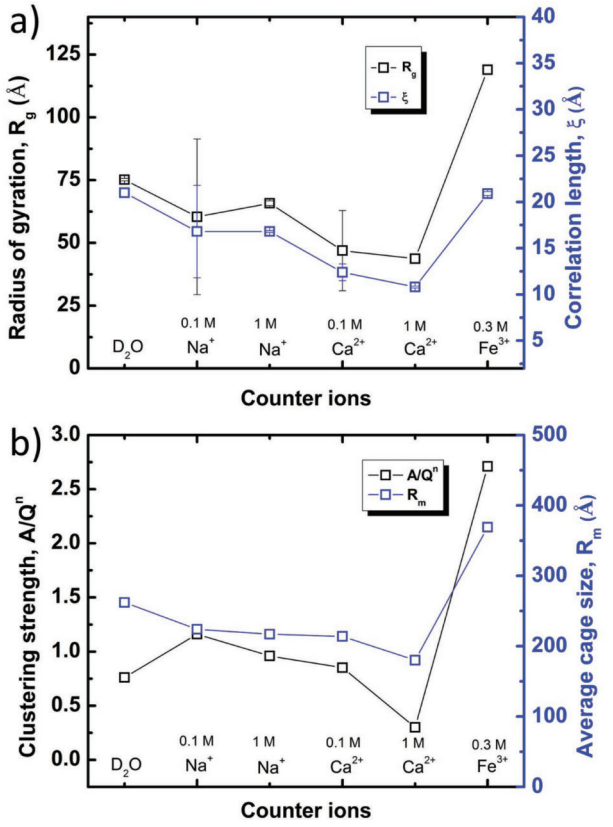

Figure 7. Parameters of Gelatin hydrogels in D_2O with different concentration and counter ion valence obtained from the SANS/VSANS fitting results by Equations (2) and (5). a) Radius of gyration and correlation length obtained from "Regime II." b) The clustering strength, A/Qn (Q = 0.02 $Å^{-1}$) and the average cage size of the hydrogels, R_m.

structuring effect to the network by providing more crosslinks between the gelatin network chains and through metal ligand interactions. This enhanced crosslinking strongly improved the gel mechanical properties.

3.5. Mechanical Properties

The mechanical properties of gelatin hydrogels are greatly dependent on the physical interaction and the degree of crosslinking of the gelatin molecule. The different inter and intra molecular interactions of the gelatin molecules result in different network structures, which change the mechanical properties of the hydrogels. Rheological studies were carried out on gelatin hydrogels and gels in the presence of different metal ions. The angular frequency dependence of the storage modulus G' and loss modulus G'' is presented in **Figure 8**.

In Figure 8a, the storage modulus and loss modulus are relatively independent of the angular frequency in range from 0.1 to 500 s^{-1}. These hydrogels are typical viscoelastic materials exhibiting G' that is one order of magnitude higher than G''.[48] The storage modulus decreases with the NaCl concentration. This indicates that a change on the electrostatic interaction influences the hydrogel mechanical properties. Figure 8b compares the rheological properties of the gelatin hydrogel and

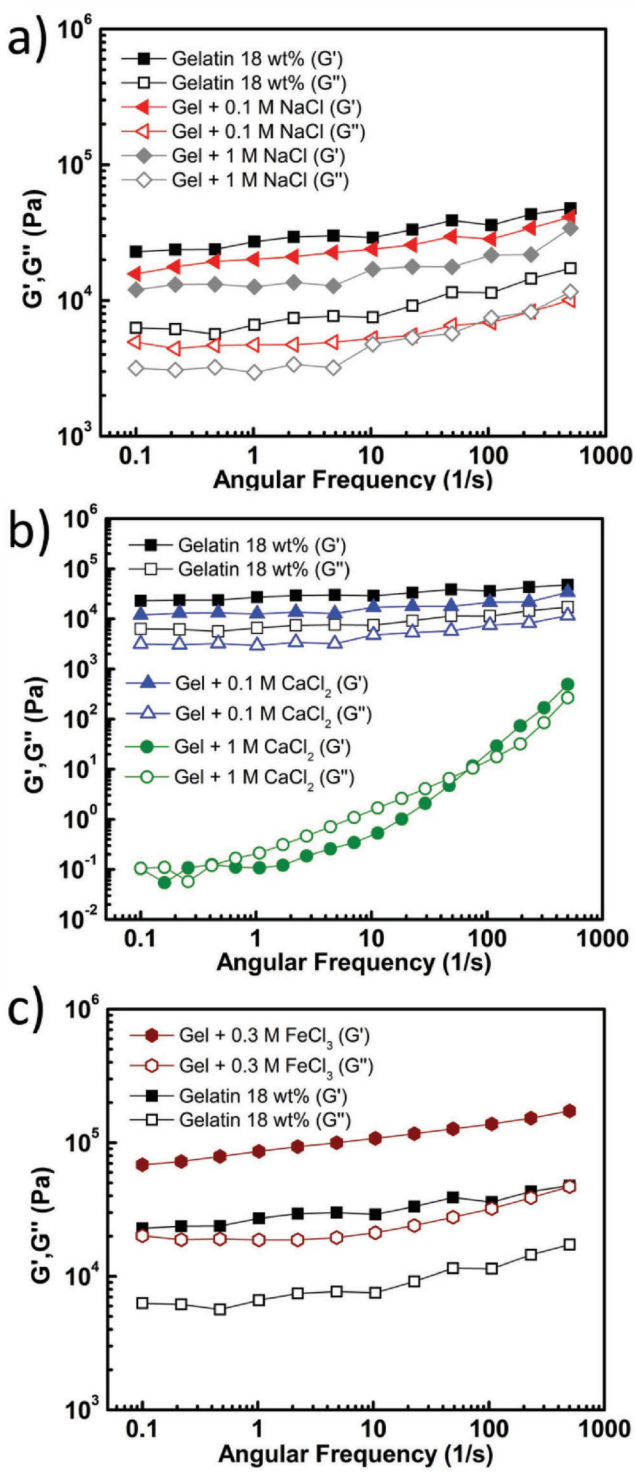

Figure 8. Comparison of storage G' and loss G'' moduli of gelatin hydrogels with different metal ions: a) 0.1 M with additional 0.1 M NaCl and 1 M NaCl, b) 0.1 M $CaCl_2$ and 1 M $CaCl_2$, c) gelatin sample (18 wt%) swollen in 0.3 M $FeCl_3$ solutions.

gels with different Ca^{2+} concentrations. The results show that G' is decreased in the presence of low Ca^{2+} concentration. The hydrogels in the presence of larger Ca^{2+} concentration (1 M)

show the behavior of a viscous solution like G' with a higher G'' than G' between 0.5 and 100 s^{-1}. These results are consistent with the SANS experiments showing that the loss of a rigid network in the presence of 1 M Ca^{2+} is resulting in poor mechanical properties. With the addition of Fe^{3+} to the hydrogels, G' becomes one order of magnitude higher than in pure gelatin hydrogels indicating the significant strengthening of the gelatin gel (Figure 8d). Rheology and SANS results confirm that gelatin hydrogels show the best structural enhancement by adding Fe^{3+} ions.

3.6. Swelling Properties

The swelling ratio (S_d) has been widely used as a simple method to characterize water absorption and stability of hydrogels. In addition, the swelling degree is associated to the crosslinking density as treated for example in the Flory–Rehner theory.[49] The swelling behavior of gelatin hydrogels (18 wt%) in deionized water and different salt solutions as a function of time is depicted in **Figure 9**. All samples have reached an equilibrium swelling after 150 h at room temperature (20 ± 2 °C). For hydrogel swelling in 1 M $CaCl_2$, the gel will dissolve in the salt solution after 24 h indicating that Ca^{2+} has the ability to break the gel network. Hydrogels in 1 M NaCl have the highest swelling ratio of 230% in 150 h, while in deionized water the swelling ratio is less than 50%. The gel swelling in 0.1 M $CaCl_2$ is higher than in 0.1 M NaCl, which may be due to the different ionic strength. The hydrogels in Fe^{3+} ion solutions show distinguished swelling properties in comparison with other solvents. At the early stages (1 h), the swelling ratio development was negative (≈–8%), the ratio becomes positive after being in iron solutions for more than 6 h and finally the hydrogels reached a ratio of ≈110%. The reason for the early time negative swelling is caused from the iron induced crosslinking of the gelatin molecules. The final positive swelling in the presence of Fe^{3+} ions may be caused by the hydrolysis of Fe^{3+} ions or the intermedium products. This process broke the crosslinking points which crosslinked by iron ions in the gels. Without the crosslinking effect, the hydrogel continues swelling until it reaches the equilibrium value.

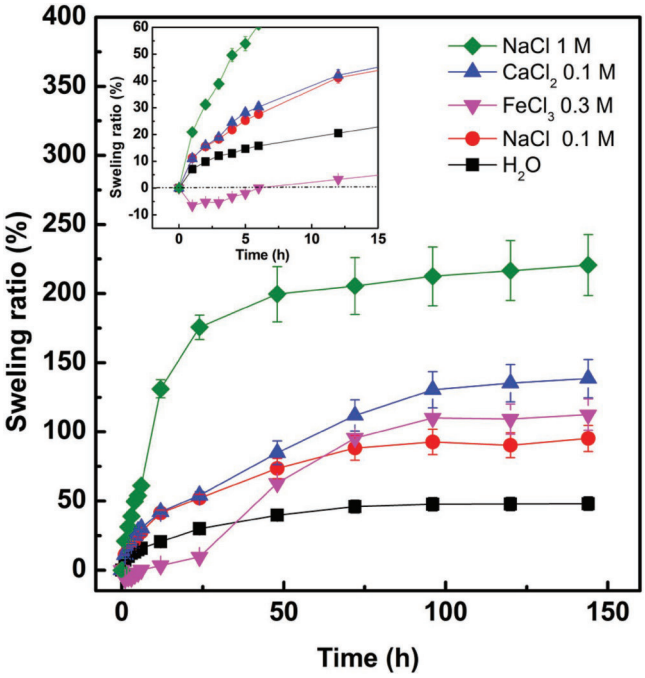

Figure 9. Mass based swelling ratios of gelatin hydrogels (gelatin 18 wt%) in the presence of different metal ions.

4. Conclusions

In this work, the ion dependence of gelatin hydrogel structure has been investigated by small and very small angle neutron scattering, which is well described by a multilevel model. On the small length scale level of the hydrogel structure, the variation of external parameters such as gelatin concentration, pH, or addition of different metal ions affect the conformational state of the gelatin molecule, the physical interaction, and crosslinking. In the gelatin hydrogels, triple helices are more efficient achieving a higher stiffness of the networks. Trivalent ions have a high ability to enhance triple-helix conformations and the degree of crosslinks through metal ligand interactions in the gelatin molecules, which strongly improve the gel mechanical properties. Divalent ions have the ability to deform the gelatin triple-helix gel network at higher salt concentrations. Thus, metal ions remarkably change the gelatin molecule interchain and intrachain physical/chemical interactions, which have a strong impact on a stiffer structure. On the large length scale level, addition of protons (lower pH) or mono/divalent ions have no significant influence on the size of the dispersed gelatin clusters. Higher charge ions (Fe^{3+}) or less protons (higher pH) increase the crosslinks thereby favoring aggregation of large clusters in the gel network structure. The aggregation of the larger clusters directly correlates with a higher stiffness of the networks.

Overall, the systematic investigation presented here yields detailed structural and mechanistic information on gelatin hydrogels in the presence of different additives and, in particular, their ability to tune the gel structure by adding metal ions. This knowledge should help to better control the hydrogel structure and stability for biomedical applications that require higher stiffness and water resistance.

Acknowledgements

This work was supported by the Deutsche Forschungsgemeinschaft within the priority program SPP 1569 "Generation of Multifunctional Inorganic Materials by Molecular Bionics."

Conflict of Interest

The authors declare no conflict of interest.

Keywords

gelatin hydrogels, ionic dependence, SANS, VSANS

[1] X. L. Zhao, D. Yamazaki, S. Kakizawa, Z. Pan, H. Takeshima, J. J. Ma, *Channels* **2011**, *5*, 389.
[2] A. Hagenston, M. Simonetti, *Cell Tissue Res.* **2014**, *357*, 407.
[3] C. Sissi, B. K. Cheng, V. Lombardo, Y. C. Tse-Dinh, M. Palumbo, *Gene* **2013**, *524*, 253.
[4] M. Djabourov, *Contemp. Phys.* **1988**, *29*, 273.
[5] M. Djabourov, *Polym. Int.* **1991**, *25*, 135.
[6] K. Okuyama, X. Z. Xu, M. Iguchi, K. Noguchi, *Biopolymers* **2006**, *84*, 181.
[7] D. A. Prystupa, A. M. Donald, *Polym Gels Networks* **1996**, *4*, 87.
[8] H. B. Bohidar, S. S. Jena, *J. Chem. Phys.* **1993**, *98*, 8970.
[9] G. I. Bourdygina, P. V. Kozlov, *Eur. Polym. J.* **1992**, *28*, 135.
[10] T. Herning, M. Djabourov, J. Leblond, G. Takerkart, *Polymer* **1991**, *32*, 3211.
[11] I. Pezron, M. Djabourov, J. Leblond, *Polymer* **1991**, *32*, 3201.
[12] W. Schuurman, P. A. Levett, M. W. Pot, P. R. van Weeren, W. J. A. Dhert, D. W. Hutmacher, F. P. W. Melchels, T. J. Klein, J. Malda, *Macromol. Biosci.* **2013**, *13*, 551.
[13] H. Shin, B. D. Olsen, A. Khademhosseini, *Biomaterials* **2012**, *33*, 3143.
[14] M. L. Smith, K. Heitfeld, C. Slone, R. A. Vaia, *Chem. Mater.* **2012**, *24*, 3074.
[15] J. Y. Lai, *J. Mater. Sci.: Mater. Med.* **2010**, *21*, 1899.
[16] S. Ullm, A. Kruger, C. Tondera, T. P. Gebauer, A. T. Neffe, A. Lendlein, F. Jung, J. Pietzsch, *Biomaterials* **2014**, *35*, 9755.
[17] M. Zandi, H. Mirzadeh, C. Mayer, H. Urch, M. B. Eslaminejad, F. Bagheri, H. Mivehchi, *J. Biomed. Mater. Res., Part A* **2010**, *92A*, 1244.
[18] Q. Xing, K. Yates, C. Vogt, Z. Qian, M. C. Frost, F. Zhao, *Sci. Rep.* **2014**, *4*, 4706.
[19] D. E. Perea, J. Liu, J. Bartrand, Q. Dicken, S. T. Thevuthasan, N. D. Browning, J. E. Evans, *Sci. Rep.* **2016**, *6*, 22321.
[20] J. B. Hayter, J. Penfold, *Mol. Phys.* **1981**, *42*, 109.
[21] J.-P. Hansen, J. B. Hayter, *Mol. Phys.* **1982**, *46*, 651.
[22] R. Z. Kramer, J. Bella, P. Mayville, B. Brodsky, H. M. Berman, *Nat. Struct. Biol.* **1999**, *6*, 454.
[23] M. A. da Silva, F. Bode, I. Grillo, C. A. Dreiss, *Biomacromolecules* **2015**, *16*, 1401.
[24] M. Helminger, B. Wu, T. Kollmann, D. Benke, D. Schwahn, V. Pipich, D. Faivre, D. Zahn, H. Cölfen, *Adv. Funct. Mater.* **2014**, *24*, 3187.
[25] B. A. Roeder, K. Kokini, J. E. Sturgis, J. P. Robinson, S. L. Voytik-Harbin, *J. Biomech. Eng.* **2002**, *124*, 214.
[26] M. Shibayama, *Polym. J.* **2011**, *43*, 18.
[27] A. V. Feoktystov, H. Frielinghaus, Z. Y. Di, S. Jaksch, V. Pipich, M. S. Appavou, E. Babcock, R. Hanslik, R. Engels, G. Kemmerling, H. Kleines, A. Ioffe, D. Richter, T. Bruckel, *J. Appl. Crystallogr.* **2015**, *48*, 61.
[28] V. Pipich, Z. Fu, *J. Large-Scale Res. Facil.* **2015**, *1*, A31.
[29] SANS Data Treatment Package, http://www.qtikws.de (accessed: December 2015).
[30] S. R. Kline, *J. Appl. Crystallogr.* **2006**, *39*, 895.
[31] G. Beaucage, *J. Appl. Crystallogr.* **1995**, *28*, 717.
[32] R. S. Justice, D. H. Wang, L. S. Tan, D. W. Schaefer, *J. Appl. Crystallogr.* **2007**, *40*, S88.
[33] W. S. Tung, V. Bird, R. J. Composto, N. Clarke, K. I. Winey, *Macromolecules* **2013**, *46*, 5345.
[34] J. Teixeira, *J. Appl. Crystallogr.* **1988**, *21*, 781.
[35] B. Hammouda, D. L. Ho, S. Kline, *Macromolecules* **2004**, *37*, 6932.
[36] S. B. Ross-Murphy, *Imaging Sci. J.* **1997**, *45*, 205.
[37] P. M. Gilsenan, S. B. Ross-Murphy, *Food Hydrocolloids* **2000**, *14*, 191.
[38] B. Hammouda, D. Worcestery, *Biophys. J.* **2006**, *91*, 2237.
[39] A. G. Nurul, N. M. Sarbon, *Int. Food Res. J.* **2015**, *22*, 572.
[40] C. G. B. Cole, *Encyclopedia of Food Science and Technology*, 2nd ed. (Ed: F. J. Francis), New York, Wiley **2000**, pp. 1183–1188.
[41] A. Krężel, W. Bal, *J. Inorg. Biochem.* **2004**, *98*, 161.
[42] Y. Takagishi, T. Kawakami, Y. Hara, M. Shinkai, T. Takezawa, T. Nagamune, *Tissue Eng.* **2006**, *12*, 927.
[43] W. J. Landis, R. Jacquet, *Calcif. Tissue Int.* **2013**, *93*, 329.
[44] P. Lo Nostro, B. W. Ninham, *Chem. Rev.* **2012**, *112*, 2286.
[45] M. G. Cacace, E. M. Landau, J. J. Ramsden, *Q. Rev. Biophys.* **1997**, *30*, 241.
[46] J. Bello, J. R. Vinograd, *Nature* **1958**, *181*, 273.
[47] Z. Walsh, E. R. Janecek, J. T. Hodgkinson, J. Sedlmair, A. Koutsioubas, D. R. Spring, M. Welch, C. J. Hirschmugl, C. Toprakcioglu, J. R. Nitschke, M. Jones, O. A. Scherman, *Proc. Natl. Acad. Sci. USA* **2014**, *111*, 17743.
[48] A. Ghoorchian, J. R. Simon, B. Bharti, W. Han, X. H. Zhao, A. Chilkoti, G. P. Lopez, *Adv. Funct. Mater.* **2015**, *25*, 3122.
[49] P. J. Flory, J. Refiner Jr., *J. Chem. Phys.* **1943**, *11*, 521.